JGR Oceans

RESEARCH ARTICLE
10.1029/2024JC021674

Special Collection:
The U.S. GEOTRACES Pacific Meridional Transect (GP15)

Meridional Central Pacific Ocean Depth Section for Pb and Pb Isotopes (GEOTRACES GP15, 152°W, 56°N to 20°S) Including Shipboard Aerosols

Jiang Shuo[1], Nathan Lanning[2,3], Edward Boyle[2], Jessica Fitzsimmons[3], Jahandar Ramezani[2], Avery G. Wang[4], and Jing Zhang[1]

[1]State Key Laboratory of Estuarine and Coastal Research, East China Normal University, Shanghai, China, [2]Department of Earth, Atmospheric and Planetary Sciences, Massachusetts Institute of Technology, Cambridge, MA, USA, [3]Oceanography Department, Texas A&M University, College Station, TX, USA, [4]Washington University, St. Louis, MO, USA

Key Points:

- A detailed meridional depth transect of dissolved lead (Pb) and Pb isotopes from Alaska to Tahiti has been obtained showing higher Pb in the northern hemisphere
- Australian-type low $^{206}Pb/^{207}Pb$ is seen in the northward-flowing SubAntarctic Mode Water in the southernmost stations
- $^{208}Pb/^{206}Pb$ versus $^{206}Pb/^{207}Pb$ plots show North Pacific and the equatorial upper 150 m waters fall on a Chinese versus U.S. line; South Pacific waters and Equatorial deep waters fall on a Australian versus American line

Supporting Information:

Supporting Information may be found in the online version of this article.

Correspondence to:

E. Boyle,
eaboyle@mit.edu

Citation:

Shuo, J., Lanning, N., Boyle, E., Fitzsimmons, J., Ramezani, J., Wang, A. G., & Zhang, J. (2025). Meridional central Pacific Ocean depth section for Pb and Pb isotopes (GEOTRACES GP15, 152°W, 56°N to 20°S) including shipboard aerosols. *Journal of Geophysical Research: Oceans*, *130*, e2024JC021674. https://doi.org/10.1029/2024JC021674

Received 5 AUG 2024
Accepted 17 DEC 2024

Author Contributions:

Conceptualization: Edward Boyle, Jessica Fitzsimmons
Data curation: Nathan Lanning, Jessica Fitzsimmons
Formal analysis: Jiang Shuo, Nathan Lanning, Edward Boyle, Jessica Fitzsimmons, Jahandar Ramezani, Avery G. Wang
Funding acquisition: Edward Boyle, Jessica Fitzsimmons
Methodology: Edward Boyle, Jessica Fitzsimmons, Jahandar Ramezani

Abstract Most oceanic lead (Pb) is from anthropogenic emissions into the atmosphere deposited into surface waters, mostly during the past two centuries. The space- and time-dependent emission patterns of anthropogenic Pb (and its isotope ratios) constitute a global geochemical experiment providing information on advective, mixing, chemical, and particle flux processes redistributing Pb within the ocean. Pb shares aspects of its behavior with other elements, for example, atmospheric input, dust solubilization, biological uptake, and reversible exchange between dissolved and adsorbed Pb on sinking particles. The evolving distributions allow us to see signals hidden in steady-state tracer distributions. The global anthropogenic Pb emission experiment serves as a tool to understand oceanic trace element dynamics. We obtained a high-resolution (5° station spacing) depth transect of dissolved Pb concentrations and Pb isotopes from Alaska (55°N) to just north of Tahiti (20°S) near 152°W longitude. The sections reveal distinct sources of Pb (American, Australian, and Chinese), transport of Australian style Pb to the water mass formation region of Sub-Antarctic Mode Water which is advected northward, columnar Pb isotope contours due to reversible particle exchange on sinking particles from high-productivity particle veils, and a gradient of high northern deep water [Pb] to low southern deep water [Pb] that is created by reversible exchange release of Pb from sinking particles carrying predominantly northern hemisphere Pb. $^{208}Pb/^{206}Pb$ versus $^{206}Pb/^{207}Pb$ isotope relationships show that most oceanic Pb in the North Pacific is from Chinese and American sources, whereas Pb in the South Pacific is from Australian and American sources.

Plain Language Summary Humans have increased the flux of lead (Pb) into the atmosphere by a factor of 20. Most of this lead is deposited in the ocean, where it is dispersed by currents, mixing, and interactions with sinking particles. The intensity and sources of lead have changed strongly with time. Using lead isotopes, we can distinguish between American, Australian, and Chinese lead. We measured lead and its isotope ratios on seawater samples from a North-South section in the central Pacific Ocean (152{degree sign} W). We find that most of the lead in the North Pacific Ocean today is from China with a significant residual component of American lead from previous emissions. South of the equator, most of the lead is a mixture of Australian and American lead, with a particularly strong Australian component at 10–20{degree sign}S in the northward-spreading SubAntarctic Mode Water. This seawater data is consistent with atmospheric aerosol data collected along the research cruise track.

1. Introduction

Lead (Pb) is the most dispersed elemental contaminant in the earth surface geochemical system (Nriagu, 1989; Patterson & Settle, 1987a). Lead is emitted into the atmosphere by industrial processes (smelting, high temperature combustion) and by automotive and aeronautical fuels with tetraethyl Pb additives being dispersed globally extending to the most remote places. Volcanoes can contribute a small natural source into the atmosphere (Patterson & Settle, 1987b) and weathering of natural minerals contributes a small amount into the hydrosphere; however, both of the latter sources are small compared to the anthropogenic mobilization. Anthropogenic Pb is dispersed globally and can be found in the most remote places (McConnell et al., 2002, 2014). With four stable isotopes, three of which are radiogenic products of the ^{238}U, ^{235}U, and ^{232}Th decay series, different geological ore deposits can be differentiated depending on the temporal history of their source Pb rocks and their U/Pb and Th/Pb ratios. Because Pb is highly recycled, different regions tend to acquire persistent characteristics that allow

Project administration: Edward Boyle, Jessica Fitzsimmons
Resources: Edward Boyle, Jing Zhang
Software: Edward Boyle
Supervision: Jessica Fitzsimmons, Jing Zhang
Validation: Edward Boyle, Jessica Fitzsimmons, Jahandar Ramezani
Visualization: Edward Boyle, Jahandar Ramezani
Writing – original draft: Jiang Shuo, Edward Boyle
Writing – review & editing: Jiang Shuo, Nathan Lanning, Jessica Fitzsimmons, Jahandar Ramezani, Jing Zhang

differentiation between sources: for example, one can distinguish American Pb from European Pb, South Asian and Australian Pb from U.S. Pb, and Chinese Pb from North and South American and Australian and South Asian Pb. Because emissions have evolved on decadal and centennial time scales, Pb is behaving as a large-scale global experiment on ocean chemistry, where fluxes from the atmosphere into the surface ocean are dispersed by ocean circulation and sinking particle transport pathways. The goal of the International GEOTRACES program is to map out the global distribution of trace elements and their isotopes in the ocean to understand how they behave biogeochemically and their uses in understanding chemical dispersal processes within the ocean. This manuscript describes the distribution of Pb concentration [Pb] and Pb isotope ratios ($^{206}Pb/^{207}Pb$, $^{208}Pb/^{206}Pb$, and $^{206}Pb/^{204}Pb$) on a North-South vertical section from Alaska to Tahiti along 152°W. This is the longest and most detailed meridional section of these properties to date passing through distinctive oceanographic and biogeochemical provinces capable of unraveling Pb sources and processes affecting Pb dispersion within the ocean.

1.1. The Central Pacific Meridional Ocean Setting

Station positions from GEOTRACES Section GP15 (USGT northern PMT) are shown in Figure 1. The track starts near Alaska, at 55°N, 158.5°W, proceeds southeast to 52.5°N, 152°W, then follows 152°W south to near Tahiti (20°S).

The cruise track passes through a great variety of oceanographic settings including: cyclonic subpolar gyres, through the anticyclonic central North Pacific subtropical gyre, across the complex zonal circulation in the equatorial region, to the northern portion of the central South Pacific anticyclonic subtropical gyre (Talley et al., 2011). Beginning with the westward flowing Alaskan Stream which receives freshwater from mountainous glaciers and passes through the subpolar gyre, the southern boundary is the high productivity Subarctic Frontal Zone (SAFZ) at ∼42°N which is part of the eastward flowing North Pacific Current. Here, surface currents upwell nutrients stimulating high biological productivity. The center of the North Pacific Subtropical Gyre has low nutrients and low productivity. The equatorial region has alternating eastward and westward flows: westward North Equatorial Current (8–20°N), eastward North Equatorial Counter Current (∼5°N), westward South Equatorial Current (3°N to 10°S) including Ekman divergence induced upwelling at the equator underlain by the eastward flowing Humboldt Equatorial Undercurrent. Southward, the anticyclonic South Pacific Subtropic Gyre has low nutrients and low biological productivity.

In the deeper ocean, the intermediate water is fed by North Pacific Intermediate Water formed in the Sea of Okhotsk in winter. The densest water arrives from the Antarctic as Circumpolar Deep water, and returns southward as Pacific Deep Water. The inflow of Circumpolar Deep Water is topographically constrained with some abyssal water passing through a narrow passageway south of Hawaii into the Eastern Deep Pacific (Edmond et al., 1971) and most water flowing northward west of Hawaii (Kawabe & Fujio, 2010; Reid, 1997).

1.2. Pb Sources to the Central Pacific and Pb Residence Times

Pre-anthropogenic Pb inputs to the northern Pacific Ocean, as represented by sea floor surface sediments, have a predominantly "crustal" $^{206}Pb/^{207}Pb$ ratio from about 1.184 to 1.196 (Chow & Patterson, 1962), reflecting continentally derived sediments and submarine hydrothermal Pb near the ridge crests (Chen et al., 1986), with the lower values reflecting a larger proportion of subduction zone volcanic Pb. Wu et al. (2010) proposed that reversible scavenging of Pb between sinking crustal particles and seawater set the deep water Pb isotope composition to these values and that in the deepest Pacific there is still a substantial pre-anthropogenic reservoir with this isotopic composition.

In anthropogenic times, Pb was most substantially contributed by leaded gasoline emissions with the U.S. being the predominant source (Boyle et al., 2014). Although U.S. $^{206}Pb/^{207}Pb$ isotope ratios have varied in time and space, they generally fell in the range 1.18–1.20 during the period of leaded gasoline emissions (Kelly et al., 2009). Flegal et al. (1984) measured surface water $^{206}Pb/^{207}Pb$ isotope ratios of 1.196 in 1980 from a central Pacific site (15°N, 158°10'W) which is consistent with U.S.-sourced lead being the dominant source to the North Pacific Ocean during this period. Since this is not significantly different from the pre-anthropogenic ratio, the enhanced Pb source derived from sinking particles would not have significantly changed deep Pb isotope ratios during this period although it would have increased deep ocean Pb concentrations. As the U.S., Canada, and Japan phased out leaded gasoline beginning in the 1980's, the dominant Pb source shifted to China (Flegal et al., 2013),

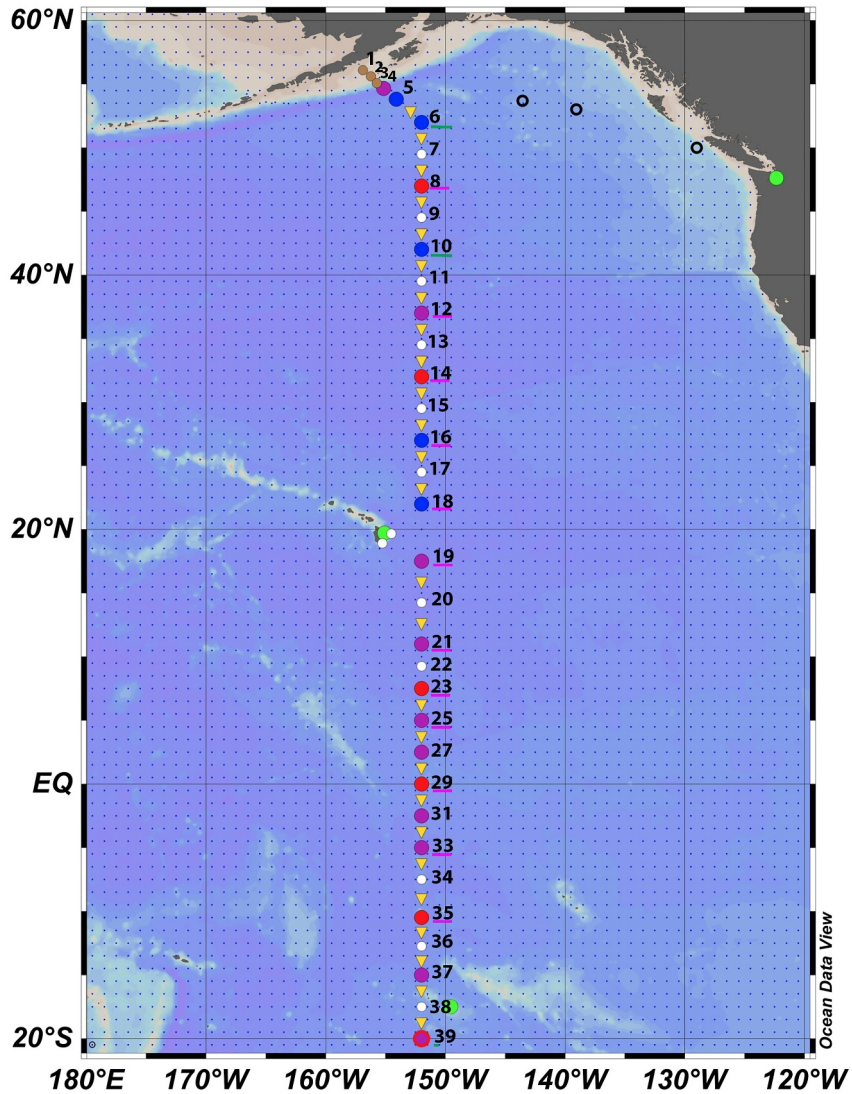

Figure 1. GEOTRACES GP15 cruise track. Green circles: ports, open black circles: rinse stations, brown circles: shelf and slope stations, purple circles: full 36-depth stations, blue circles: full 24-depth stations, white circles: 1,000 m demi stations, yellow triangle: intermediate fish samples.

with lower $^{206}Pb/^{207}Pb$ isotope ratios of ~1.155 (Boyle et al., 2020; Pinedo-Gonzalez et al., 2018). This Pb can be recognized by its higher $^{208}Pb/^{206}Pb$ ratio at a given $^{206}Pb/^{207}Pb$ value (Ewing et al., 2010).

The residence time of Pb in the surface ocean depends on the biological productivity of the region. Nozaki et al. (1976) mapped out the distribution of ^{222}Rn-derived ^{210}Pb in surface waters of the Pacific Ocean and found that it varied in activity from 7 to 25 dpm/100 kg, with the lowest values near the highest latitudes, equator, and western and eastern boundaries. The highest values are seen in the central North Pacific Gyre. Assuming a longitudinal ^{210}Pb deposition flux variation across the Pacific, they estimated that the Pb residence time in the central North Pacific Gyre is 1.7 years.

In deep waters, ^{210}Pb scavenging onto sinking particles is indicated by $^{210}Pb/^{226}Ra$ activity ratios of ~0.5, signifying a scavenging residence time of about 30 years (Chung et al., 1983). Since it takes about 1,000 years for surface water to flush the deep North Pacific (Matsumoto, 2007), the amount of advective Pb carried from source surface waters is negligible in the deep Pacific. However, in particle-rich environments such as the North and Equatorial Pacific particle veils, anthropogenic Pb isotope signatures can be observed throughout the entire water column perturbing the natural deep Pacific Pb cycle (Lanning et al., 2023).

2. Materials and Methods

2.1. Seawater Analyses

The threads of 2 L Nalgene® high-density polyethylene bottles were leached in reagent grade 2M HCl for one day before the bottles were filled with reagent grade 1M HCl and leached for 24 hr at 60°C. The bottles were then inverted and allowed to stand for one more day. The bottles were rinsed 3 times with high-purity distilled water, then refilled with high-purity 0.001 M HCl and leached for 24 hr at 60°C. The bottles were then rinsed five times with high purity distilled water, double-bagged in polyethylene, and stored in Rubbermade® totes for shipping and fieldwork.

Samples were collected on cruises RR1814 and RR1815 of the *R/V Roger Revelle* (U.S. GEOTRACES GP15) Surface water samples were collected by pumping from a "fish" towed over the side of the ship while depth profile samples were collected using the trace metal clean GO-Flo sampling rosette maintained by Greg Cutter following standard practices (Cutter & Bruland, 2012). Once samples were brought onboard, subsampling at the operationally defined dissolved cutoff (0.2 μm) was done in a positive pressure HEPA-filtered air van. Bottles were rinsed three times with samples before filling. They were then rebagged and stored in the totes until returned to the MIT where they were acidified with 4 mL of 6M optima-grade HCl and allowed to sit for months before analyzing.

Pb concentrations at three stations (8, 18, and 35) were analyzed at MIT for intercalibration with the TAMU lab which analyzed all stations. MIT used a modification of the Lee et al. (2011) ^{204}Pb isotope dilution batch method with the NTA solid-phase extractant beads replaced with Nobias Chelate PA1 beads (Sohrin et al., 2008). The extracted Pb was analyzed for ^{208}Pb/^{204}Pb on a PQ2+ quadrupole inductively coupled plasma mass spectrometer. TAMU analyzed Pb concentrations using a modified automated offline Elemental scientific SeaFAST® pico metal extraction system with Nobias Chelate PA1 resin (Jensen et al., 2020; Lagerström et al., 2013). Isotope dilution was employed to analyze [Pb] with samples buffered to a pH ∼ 6.2. Once the samples were eluted with 10% optima grade nitric acid (HNO_3) a 25× preconcentration factor by the SeaFAST [Pb] was analyzed on a Thermo Element XR high resolution inductively coupled plasma mass spectrometer at the R. Ken Williams Radiogenic Laboratory at TAMU. Data quality for Pb was assessed by direct intercalibration between MIT and TAMU on parallel samples from three stations (8, 18, and 35) with good agreement (SI figure 1 in Supporting Information S1). It was also assessed by a crossover station from the Japanese GEOTRACES cruise GEOTRACES GP (KH-17-3), station CL09 (47°N, 152°W) (Chan et al., 2024) and GP15 station 8 (47°N, 152.665°W) (SI Figure 2 in Supporting Information S1), with good agreement between the three labs. In general, the Pb concentration precision should be a few percent of the value except at the low pmol/kg levels where it may increase to ±0.5 pmol/kg.

Seawater Pb isotope ratios were measured by IsoProbe magnetic sector plasma mass spectrometry at MIT after extraction and purification of Pb using modifications of the methods described by Reuer et al. (2003) and Boyle et al. (2012). The modifications concerned Pb extraction from seawater by three different methods. Most of the southern samples were extracted using the PA1 batch extraction method described by Boyle et al. (2020). Most of the northern samples were extracted using $Mg(OH)_2$ coprecipitation, followed by dissolution in the minimal amount of 6 M high purity HCl (5–20 mL) diluted to 45 mL with high-purity distilled water, buffering to pH 5–6 using high purity ammonium acetate, and two consecutive batch solid phase extractions onto PA1 resin (Lanning et al., 2023). For station 37 only, Pb was extracted directly onto a PA1 resin mini-column after buffering to pH 4–5. For all of the stations, Pb was extracted from the resin with 0.1 M HNO_3, the solutions were dried down, and then they were purified further using AG1-X8 anion exchange using HBr-HCl binding and elution chemistry (Reuer et al., 2003).

The Pb isotope precision depends on the signal level on the mass spectrometer because of the Johnson resistor noise, about 11 μvolts for a 10 s reading. Well above that level (0.2–1.1 V), two sigma standard error values ($n = 40$) for ninety-eight 1,000 μL replicates of a laboratory standard containing 70 nmol kg^{-1} were reproducible to ^{206}Pb/^{207}Pb = 300 parts per million (ppm) and ^{208}Pb/^{207}Pb = 400 ppm. Precisions for ^{206}Pb/^{204}Pb, with the much less abundant 204 measured on a Daly style ion counter are lower, ∼2,000 ppm. For samples with low signal strengths due to low concentrations or poor recovery efficiencies during purification, errors are larger; we exclude values for ^{206}Pb/^{207}Pb that have within-run 2 s. e. > 3,000 ppm. The two sigma internal standard error values for each data point is listed in Supporting Information S1 data table. In general, we can obtain usable Pb isotope data from 1 kg samples with ≥2 pmol/kg.

For Pb isotopes, we have participated in several intercalibration exercises that are largely reviewed in Boyle et al. (2020). In addition, further information will be available from the GEOTRACES IDP2025 in its intercalibration report. There also is a crossover station for Pb isotopes at 10.5°S 152°W (GP16 EPZT station 36, -Dec. 2013 and GP15 PMT station 35 Nov. 2018) (SI Figure 3 in Supporting Information S1). The profiles are reasonably consistent; however, because Pb is an evolving time-and-space-dependent transient, these temporally displaced data cannot provide the best assessment of sampling and analysis consistency.

2.2. Aerosol Analyses

During the transits, Clifton Buck and Chris Marsay deployed automated aerosol samplers on the flying bridge, which pumped air through sterile membrane filter discs for periods of time ranging from 31.2 to 60.1 hr. These correspond to sampled volumes of air ranging from 185.0 to 357.8 cubic meters. The samplers were automated to only pump air when the wind was toward the ship, to avoid contamination from the ship exhaust. The samplers collected multiple sub-samples with the same air volumes passing through. They generously shared splits of 10 samples. These samples were leached by 0.1 M HNO_3 at 100°C for 24 hr to remove surface-bound Pb. The resulting solutions were spiked with ^{205}Pb, purified by anion exchange chromatography and analyzed for total Pb and Pb isotope ratios by thermal ionization mass spectrometry in the MIT Isotope Laboratory. Concurrently measured filter disc Pb blanks ranged from 32 to 88 pg, well below the Pb content of the analyses (0.6–11.8 ng). A parallel analysis for total Pb (processed with concentrated HNO_3 and HF, hence total Pb) on six splits of these samples (Marsay et al., 2022) showed good agreement with a single obviously contaminated split for one sample (SI Figure 4 in Supporting Information S1).

3. Results and Discussion

3.1. Features of the Seawater [Pb] and Pb Isotope Sections

The dissolved Pb concentrations ([Pb]) and Pb isotope ratios of seawater are shown as contoured sections in Figure 2, and as individual profiles in Figures 3–5. The nearest-surface water [Pb] variability and aerosol Pb concentration sample variability along the section are shown in Figures 6 and 7. Briefly, an elevated upper ocean plume of [Pb] extends from the Alaskan shelf across the Equator reaching [Pb] > 70 pmol/kg. At depths below this plume [Pb] resembles more pre-industrial concentrations; however, there is slightly elevated [Pb] in the abyssal North Pacific compared to the Equatorial Pacific (Figure 2 upper). In Pb isotope space, this high [Pb] feature is outlined by defining isotopic ratios. A northward migrating plume is seen in the southern section at ~600 m, but only in Pb isotopes not concentration, meeting the southward migrating elevated [Pb] feature (Figure 2 middle and bottom). The atmospheric aerosols show a different latitudinal pattern than the surface waters because of the different integration timescales, as discussed later in Section 3.5.

Before anthropogenic emissions, Pb in the ocean as a whole, particularly in older deep waters, occurred at low concentrations supported by weathered crustal particles carried by rivers and transported as aerosols through the atmosphere (Schaule & Patterson, 1981). In recent times (as confirmed by published work) Pb enters the ocean as particulate fallout from the atmosphere which is dominantly due to anthropogenic emissions (Marsay et al., 2022; Pinedo-Gonzalez et al., 2018; Zurbrick et al., 2017). Hence the upper ocean has higher [Pb] than older deeper waters due to source proximity. With more land area and total population, there are more anthropogenic emissions in the northern hemisphere than the southern, hence Pb in the upper northern hemisphere ocean is higher than in the southern hemisphere. Within the ocean, Pb attaches to particles that sink and reversibly exchange with deeper waters (Lanning et al., 2023; Wu et al., 2010) carried by sinking particles and released into the low-[Pb] deep waters resulting in decadal- and century-scale increasing deep water [Pb] (Wu et al., 2010). It is evident that deep [Pb] concentrations in the North Pacific are elevated compared to the Equatorial and South Pacific because the North Pacific has a higher upper ocean [Pb] resulting in higher flux of sinking particles carrying Pb to depth (Lanning et al., 2023).

In recent decades, two important changes to the atmospheric Pb flux have occurred: (a) Pb was phased out of gasoline in most countries in the world (hence most ocean surface waters now have lower [Pb] than the decade-old thermocline waters such as in the Atlantic (Boyle et al., 2014)), resulting in decreased fluxes into the surface ocean; and (b) Chinese coal combustion rose to levels where Pb emissions were even larger than they were during Chinese leaded gasoline utilization (Flegal et al., 2013). This increase has resulted in high atmospheric Pb transport from China within the westerlies maximized at ~30–40°N with our data showing a surface water [Pb]

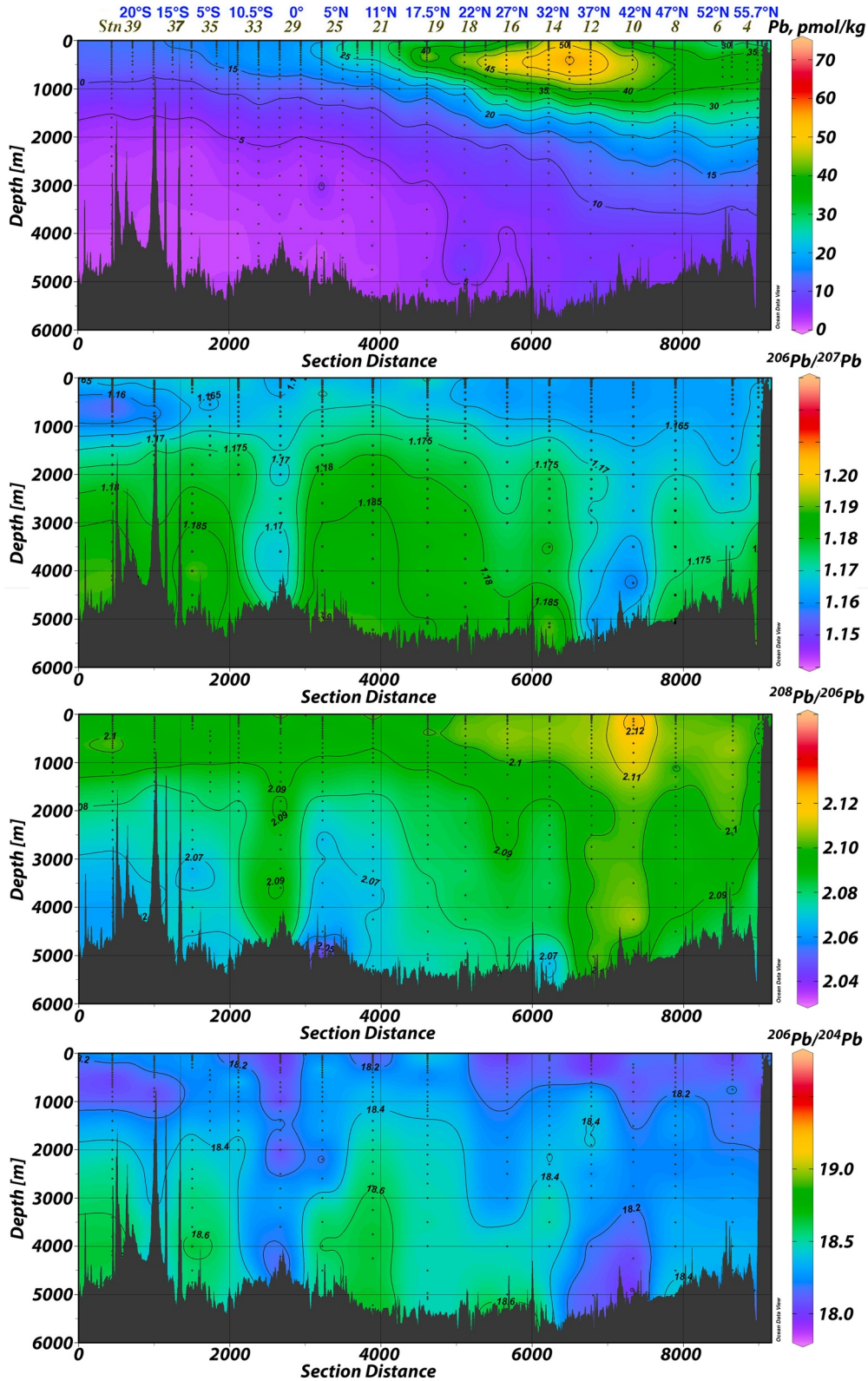

Figure 2. Dissolved Pb (upper) and $^{206}Pb/^{207}Pb$ (upper middle), $^{208}Pb/^{206}Pb$ (lower middle), and $^{206}Pb/^{204}Pb$ (bottom) sections.

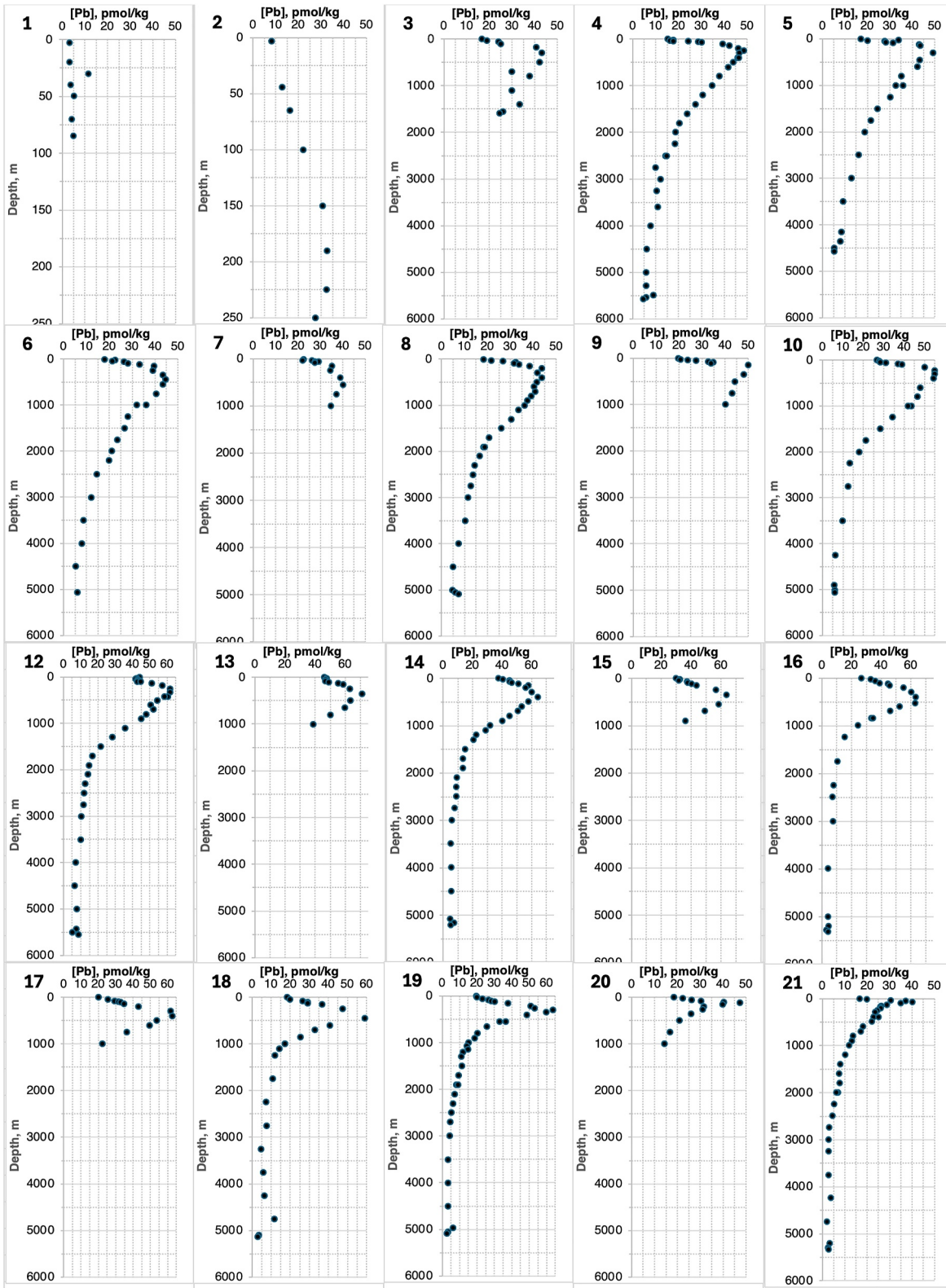

Figure 3. Vertical profiles of dissolved Pb [Pb], stations 1–21. Within-run 1 s. e. reproducibility for Pb is generally smaller than the point sizes, so error bars are not shown.

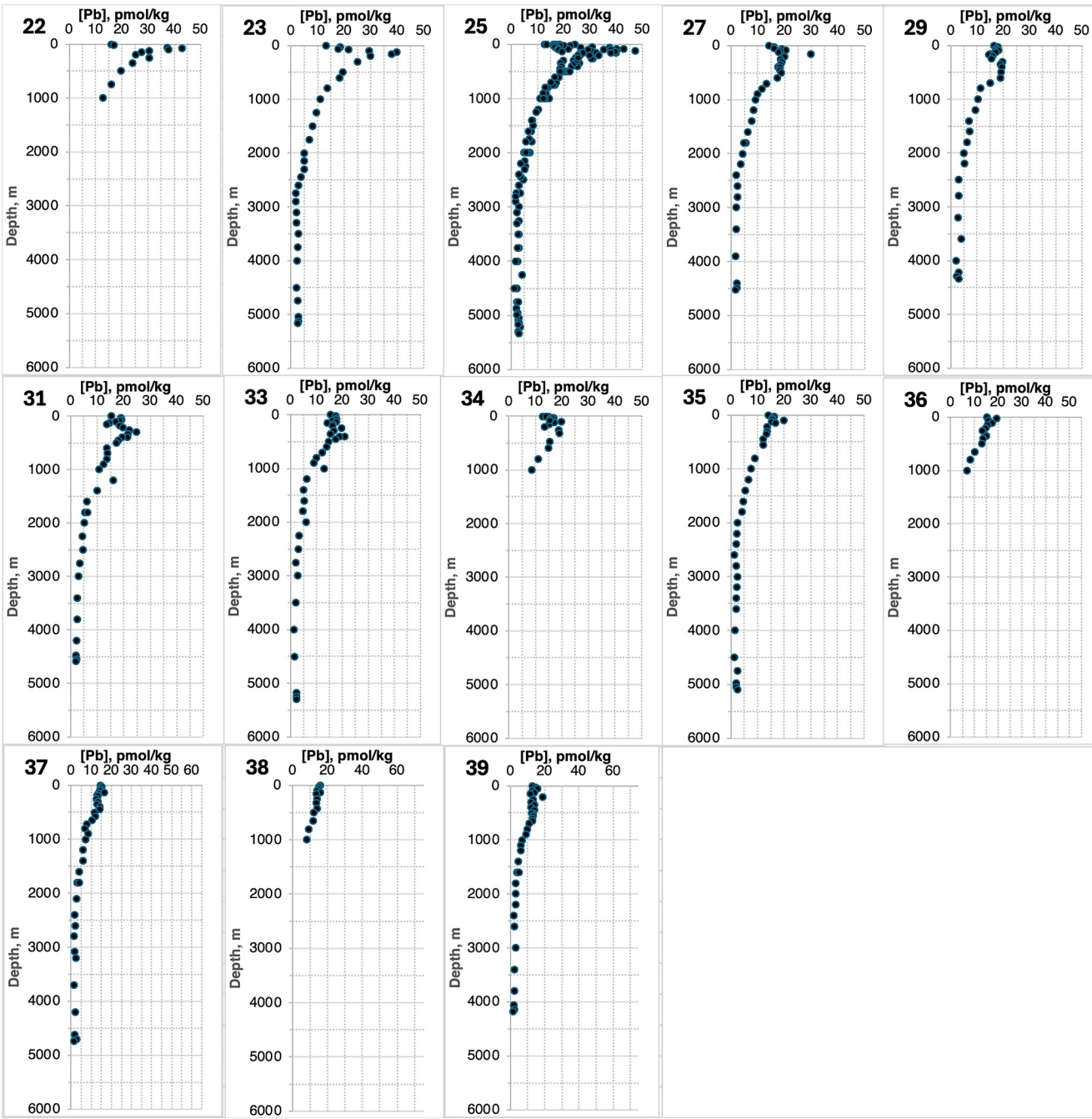

Figure 4. Vertical profiles of dissolved Pb [Pb], stations 22–39.

maximum of 43 pmol/kg at 37°N (PMT station 12; Figure 2 upper). This latitude is near the locations where winter cooling results in the subduction of surface waters (with density sigma theta ~26.7‰) into the upper thermocline, contributing additional high [Pb] water into water masses that are already elevated from having subducted during peak anthropogenic Pb emissions. This maximum spreads laterally by advection and eddy diffusion.

The consequences of these processes on Pb isotopes depends on the isotopic composition of the various sources. In pre-anthropogenic times, Pb isotopes were controlled by the isotopic composition of continental runoff Pb, which can be estimated as $^{206}Pb/^{207}Pb$ ~1.20 based on the Pb isotopic ratio of marine sediments (Chow & Patterson, 1962). Hence most of the ocean would have had this isotopic ratio, and some of this Pb from the pre-

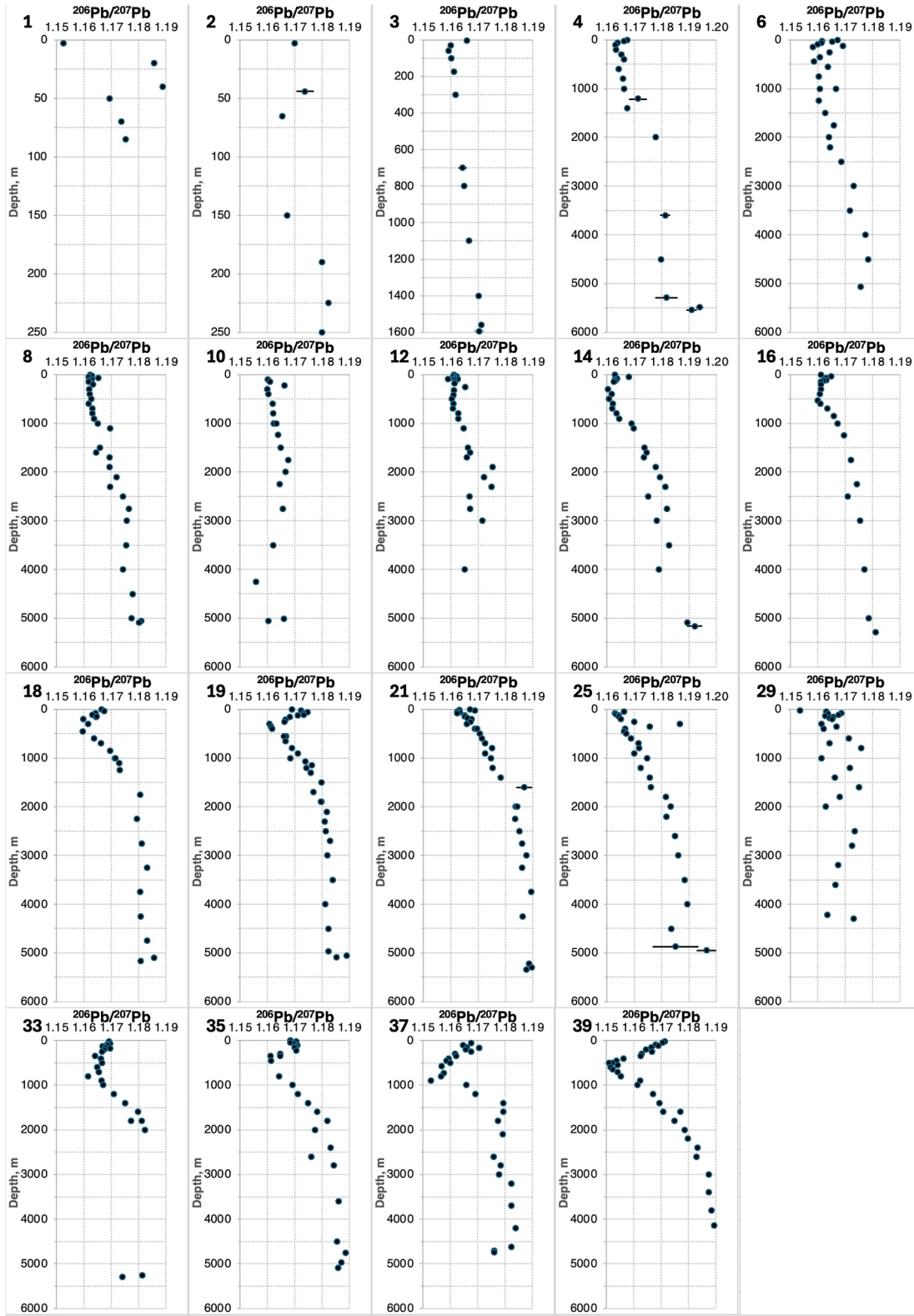

Figure 5. Vertical profiles of $^{206}Pb/^{207}Pb$. Within-run 2 s. e. reproducibility for $^{206}Pb/^{207}Pb$ is generally smaller than the point sizes, so error bars are not shown for most points, but for some samples with small Pb signals, internal 2 s. e. error bars are drawn.

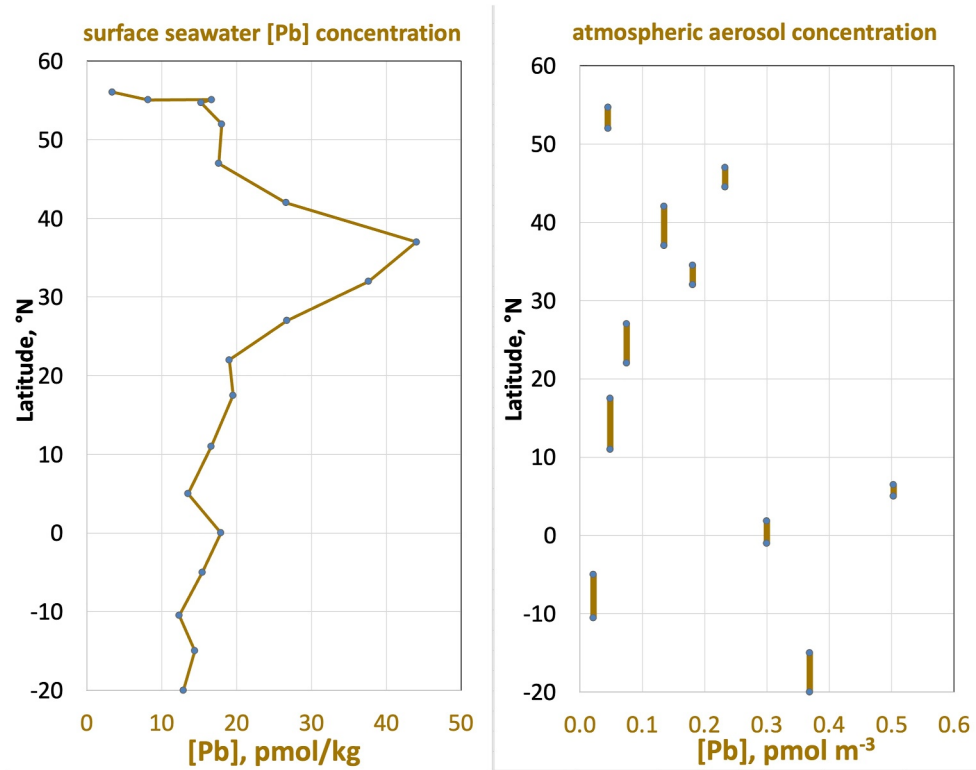

Figure 6. Near-surface dissolved Pb concentration ([Pb]), and atmospheric aerosol concentration.

anthropogenic ocean remains in the deep waters of the ocean. With the onset of anthropogenic inputs, isotopic compositions varied regionally depending on the Pb ore sources. In general, European Pb had $^{206}Pb/^{207}Pb < 1.15$ whereas American Pb (north and south) had $^{206}Pb/^{207}Pb$ of 1.17–1.22 (Boyle et al., 2014). Australian-type Pb has low $^{206}Pb/^{207}Pb$, <1.12. As the Pacific Ocean Pb sources varied from crustal (~1.20; Lee et al., 2015) to predominantly U.S.-type Pb in the northern Pacific (~1.2) and Australian-type Pb in the southern Pacific, mixing of the two sources within the ocean resulted in a linear mix between 1.20 and 1.12. As U.S. Pb gasoline was phased out and Chinese Pb (~1.16) emissions increased, upper ocean $^{206}Pb/^{207}Pb$ in the northern Pacific has decreased, while the southern Pacific Pb remained low because of the Australian-type Pb contribution. Hence the upper ocean in 2018 had lower $^{206}Pb/^{207}Pb$ than the deeper older waters (Figure 2 upper middle).

The sinking particles from the surface reversibly adsorb Pb and have been transporting it and its isotopic signature to depth during these anthropogenic periods. Hence deep Pb in the North Pacific Ocean has been slightly increasing with time (Wu et al., 2010). However, as recently noted (Lanning et al., 2023), in regions of higher

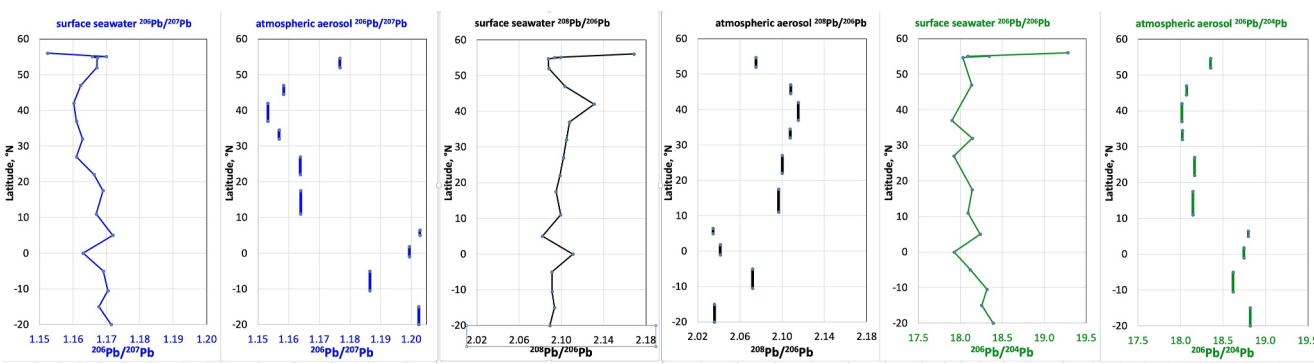

Figure 7. Surface seawater and aerosol Pb isotope data versus latitude.

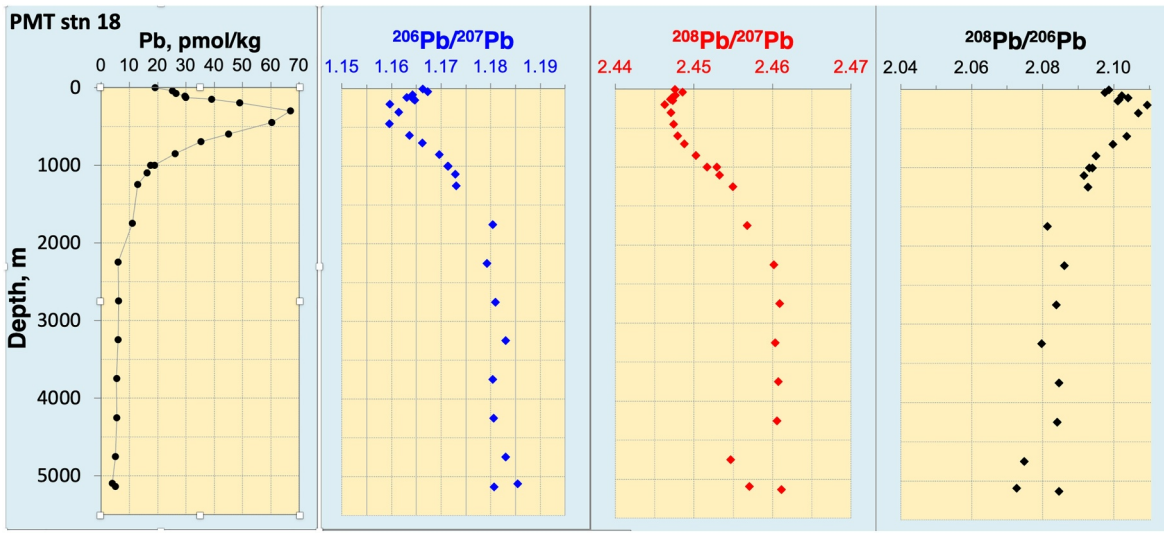

Figure 8. Vertical profiles of dissolved Pb ([Pb]) and Pb isotope data from GEOTRACES PMT station 18.

biological production due to upwelling nutrients, such as at the equator and north of 37°N, the higher flux of particles carries the anthropogenic surface water isotope ratios down throughout the entire water column at a rate sufficient to overcome horizontal mixing (Lanning et al., 2023). Our Pb isotope sections show columnar structures of isotopic ratios down from the surface to the bottom under these high productivity regions, observable in in all three independent Pb isotope ratios ($^{206}Pb/^{207}Pb$, $^{208}Pb/^{206}Pb$, and $^{206}Pb/^{204}Pb$, Figure 2).

3.2. Pb Isotope Evidence for Pacific Bottom Water Penetration Into the Eastern Pacific?

At PMT station 18 (Figure 8), two samples below 4,500 m (4,750 and 5,095 m) show different Pb isotope signatures than the water immediately above ($^{206}Pb/^{207}Pb$ = 1.1831 and 1.1855 compared to 1.1805 for the two shallower measurements above them, $^{208}Pb/^{207}Pb$ = 2.4546 and 2.4570 compared to 2.4607 above, and $^{208}Pb/^{206}Pb$ = 2.0748 and 2.0726 compared to 2.0844 above. The deepest sample (5,135 m compared to cast bottom depth of 5,175 m) returns to the shallower values: 1.1806, 2.4611, and 2.0846, perhaps as a result of release from bottom particles equilibrated during sinking through the shallower waters. We propose that this Pb isotope feature is a reflection of the topographically constrained penetration of dense Pacific Circumpolar Deep Water eastwards through a deep passage 10 km wide south of Horizon Guyot and on or around the southeastern end of the Hawaiian chain. Edmond et al. (1971) observed a maximal bottom water hydrographic anomaly of −0.3°C in temperature and +0.1‰ in salinity between 4,400 m and the bottom at 5,150 m; Kawabe and Fujio (2010) also observed some eastward transport of abyssal waters. At Station 18, the salinity only increases by +0.011‰ at 5,095 m compared to 3,750 m, so a high degree of dilution has already occurred (notably, the salinity at the deepest sample 5,135 m that does not show a Pb isotope anomaly also does not show the positive salinity anomaly, −0.020‰ compared to 3,750 m).

3.3. Australian Pb in Sub-Antarctic Mode Water (SAMW) and Antarctic Intermediate Water (AAIW)

One of the strongest features in the $^{206}Pb/^{207}Pb$ section is the minimum 1.151 seen in the upper thermocline waters of the southern two stations (37 and 39, Figure 9). The station 39,$^{206}Pb/^{207}Pb$ minimum coincides with the salinity minimum characteristic of the SubAntarctic Mode Water (SAMW, McCartney, 1977), a water mass formed near the Sub-Antarctic Front on the northern flank of the Antarctic Circumpolar Current (ACC) during winter with a sigma theta density of 26–27‰ (Bushinsky & Cerovečki, 2023; Li et al., 2021). The minimum tends to extend deeper than the formal boundary of this water mass, implying that low $^{206}Pb/^{207}Pb$ may also be found in the underlying Antarctic Intermediate Water (AAIW).

How do the Antarctic water masses become labeled with low $^{206}Pb/^{207}Pb$? We can suggest two possibilities. (a) Australian Pb is directly transported by the atmosphere to the Pacific formation waters of the ACC, particularly near their northern boundary (SAMW formation also occurs in the Indian Ocean, but may only comprise a minor

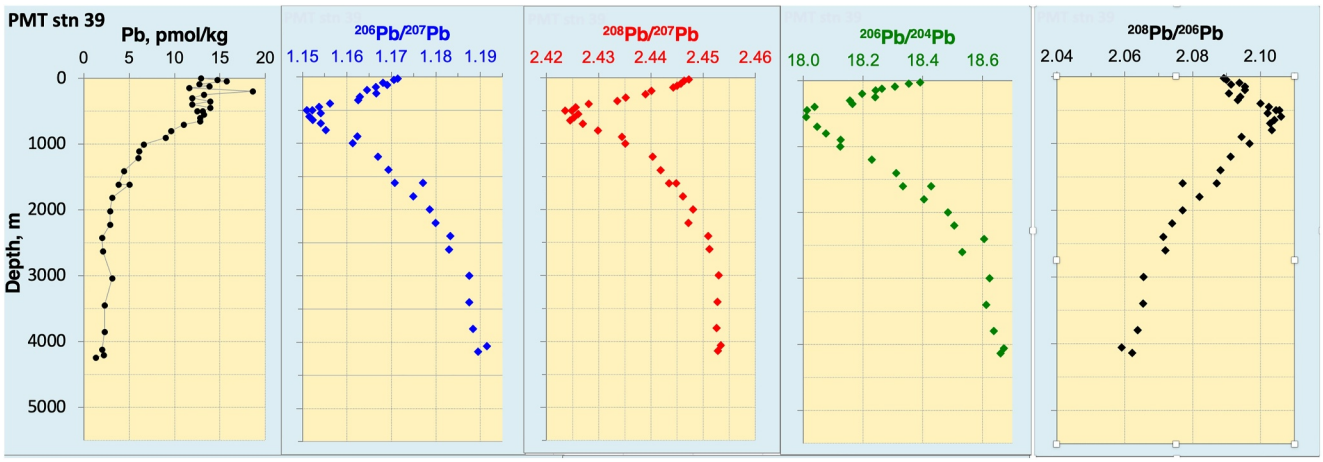

Figure 9. Vertical profiles of dissolved Pb ([Pb]) and Pb isotope data from PMT station 39.

portion in this region of the Pacific, Bushinsky & Cerovečki, 2023). NASA satellite images show that carbonaceous aerosols from eastern Australian wildfires are transported to the regions where SAMW forms (Dirksen et al., 2009; NASA, 2020; Tang et al., 2021). Given these air transport pathways, aerosol Pb from anthropogenic Australian sources (not necessarily wildfires) may be directly transported to the northern boundary of the Antarctic Circumpolar Current. (b) Low $^{206}Pb/^{207}Pb$ surface waters from the Indian Ocean may be transported by the ACC into the Pacific regions where SAMW and AABW are formed. As Lee et al. (2015) show, Pb in the upper Indian Ocean is dominated by Australian-type low $^{206}Pb/^{207}Pb$ values (~1.14–1.16). These Pb isotope ratios extend to about 40°S, where they could be incorporated into the northern ACC and brought into the Pacific formation regions of the thermocline Antarctic water masses. Further work is necessary to clarify if these possibilities can be confirmed.

3.4. Connection to Latitudinal EPZT at 10.5°S

Figure 10 illustrates the connection between our GP15 with the USGT EPZT GP16 east-west $^{206}Pb/^{207}Pb$ section at 10–16°S (Boyle et al., 2020), connecting at 10.5°S. The SAMW $^{206}Pb/^{207}Pb$ minimum extends across the GP15, becoming less evident near the South American coast. The deep waters along this E-W section do not show any particle veil effects. The deep waters below ~1,000 m have relatively uniform $^{206}Pb/^{207}Pb$ values ranging from 1.175 to slightly above 1.185, comparable to sections of the USGT PMT GP15 that are not under particle veils.

3.5. Aerosol Pb

Aerosol Pb, Pb isotope ratio, and the sampling intervals for the near-sea surface aerosols are illustrated in Figures 6 and 7. Marsay et al. (2022) show 3 day back trajectories for these samples (and include 5- and 10 day back trajectories in Supporting Information S1). There is substantial variability in total Pb (~factor of 20) with lowest concentrations (<0.1 pmol/m^3) in the northernmost sample and in the northern and southern tropics. Equatorial (0–5°N) samples showed a Pb concentration maximum. The northernmost sample (53°N) had intermediate $^{206}Pb/^{207}Pb$ (1.177) which could be influenced by Alaskan or Canadian aerosols (see discussion of Pb triple isotope features). In the rest of the northern hemisphere, $^{206}Pb/^{207}Pb$ showed low values (1.155–1.164) characteristic of Chinese anthropogenic emissions. Equatorial and southern hemisphere samples showed higher $^{206}Pb/^{207}Pb$ (1.187–1.203) characteristic of South American aerosols. Mexico and Peru are two of the 10 world's largest producers of Pb ore and much of the Pb is refined domestically (Roskill Report, 1996). Peru and Chile are the world's largest copper producers, which release lead as a by-product. The ratio of $^{206}Pb/^{207}Pb$ in Pb ore deposits ranged from 1.180 to 1.205 in Mexico and ranged from 1.199 to 1.220 in Peru (Sangster et al., 2000). The ratio of $^{206}Pb/^{207}Pb$ in Pb aerosols in two samples from Santiago Chile were 1.150 and 1.182 in 1994–1995 (Bollhöfer & Rosman, 2000).

It is evident that the surface water and aerosol Pb concentrations have significantly different latitudinal concentration variability. This observation is not surprising given the different residence time of aerosols (days to a

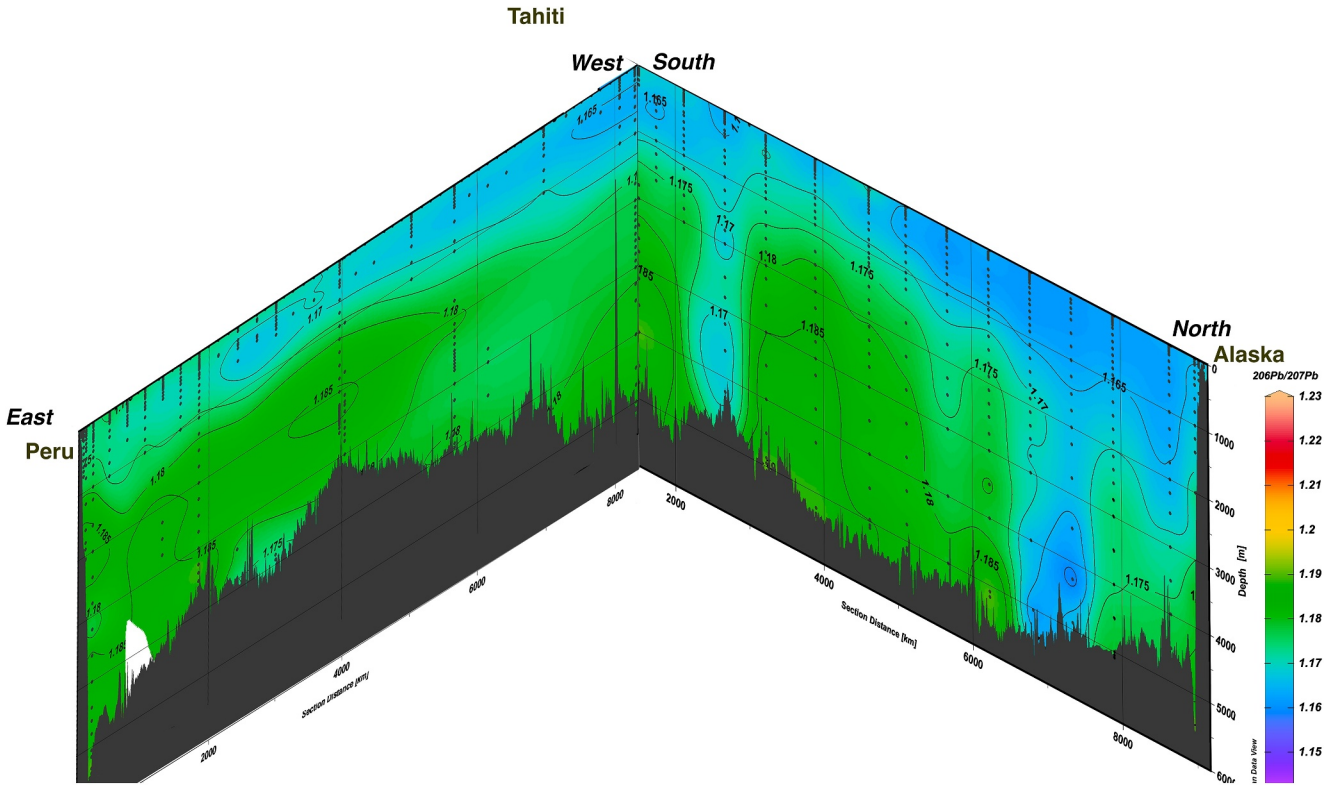

Figure 10. GEOTRACES GP16 EPZT and GP15 PMT $^{206}Pb/^{207}Pb$ sections joined together at 10.5°S, 152°W.

week) and surface water Pb (2 years), so aerosols reflect processes from a few days before sampling whereas the surface water will reflect a yearly integration of events.

3.6. Pb Triple Isotope Features

Figure 11 illustrates features that can be recognized using three isotopes, ^{206}Pb, ^{207}Pb, and ^{208}Pb. The two isotope ratios $^{206}Pb/^{207}Pb$ and $^{208}Pb/^{206}Pb$ vary between Pb ore sources because of difference in the geologic age and U/Pb and Th/Pb ratios of the source rocks. In particular, U.S. Pb has mean isotope ratios $^{206}Pb/^{207}Pb$ ~1.20 and $^{208}Pb/^{206}Pb$ ~2.05, Australian Pb has mean Pb $^{206}Pb/^{207}Pb$ ~1.1 and $^{208}Pb/^{206}Pb$ ~2.2, and Chinese Pb has $^{206}Pb/^{207}Pb$ ~1.155 and $^{208}Pb/^{206}Pb$ ~2.12. Because of these differences, a mixture of U.S. and Chinese Pb falls on a higher line on a $^{208}Pb/^{206}Pb$ versus $^{206}Pb/^{207}Pb$ plot compared to a mixture of U.S. and Australian Pb (Boyle et al., 2020; Ewing et al., 2010; Pinedo-Gonzalez et al., 2018). This Chinese-influenced Pb can be recognized by its higher $^{208}Pb/^{206}Pb$ ratio at a given $^{206}Pb/^{207}Pb$ value.

Because of the source variability combined with atmospheric transport patterns, the above source differences in the triple isotope plot depend on the latitude and depth. Most of the seawater isotope ratios at all depths from stations 2–25 fall on a Chinese-American lead line (blue and purple points). Nine out of the 10 aerosol samples also fall on this line. There are several anomalously high $^{208}Pb/^{206}Pb$ values associated with stations 1 and 10. Station 1 is a shallow station very near the Alaskan coast, probably representing something local. Station 10 is located on top of the strongest particle veil. We suggest that this feature may be due to the influence of a particularly strong high Chinese $^{208}Pb/^{206}Pb$ source, but we need other data nearer the source to know if this is correct. Most of the samples from stations 29–39 fall on an Australian-American line.

4. Conclusions

The GP15 PMT Pb and Pb isotope section is the longest and most detailed data for these properties to date emphasizing the role that Pb can play as an oceanographic tracer in this global experiment. The ocean distribution of the properties is consistent with known sources and their isotope compositions, and reversible scavenging

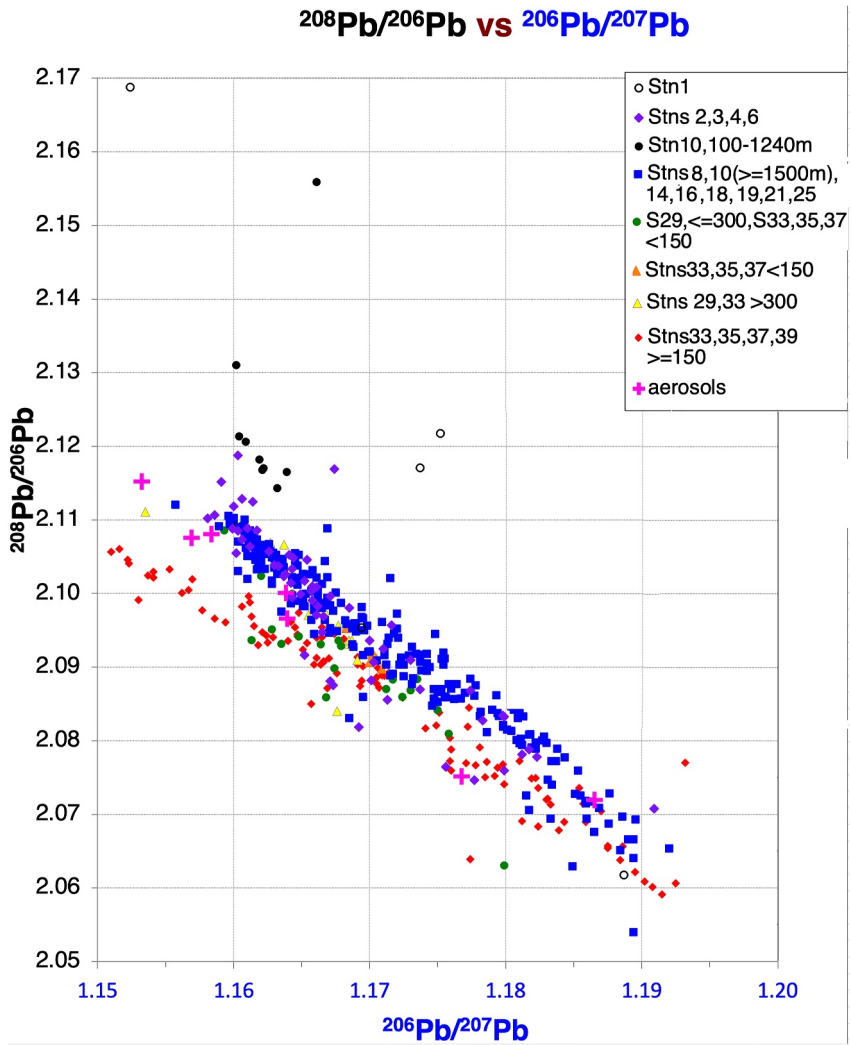

Figure 11. Triple Isotope plot of GP15 PMT $^{208}Pb/^{206}Pb$ versus $^{206}Pb/^{207}Pb$.

transporting Pb from the upper ocean to the deep sea, particularly under high productivity particle veils. Although lateral mixing and the old age of the deep waters masks advective transport, it can be seen in the low Australian $^{206}Pb/^{207}Pb$ in the Sub-Antarctic Mode Water in the southernmost stations, and in the penetration of dense Pacific Bottom Water through the passageways south of Hawaii. The GP15 PMT section connects to the GP16 EPZT section, providing a N-S and E-W three-dimensional view of the Pb isotope distribution in a key region for intermediate and deep water circulation. The aerosols collected while steaming show Chinese Pb in the northern sections and North- or South-American Pb in the southern sections. The triple isotope $^{208}Pb/^{206}Pb$ versus $^{206}Pb/^{207}Pb$ plots show that most of the North Pacific and the upper waters of the equatorial Pacific fall on a Chinese Pb versus U.S Pb line, whereas the South Pacific surface and deep waters fall on an Australian versus American Pb line demonstrating strong meridional variability in oceanic Pb sources.

Data Availability Statement

The seawater [Pb] are included in SI Table S1 in Supporting Information S1, the Pb isotope data are included in SI Table S2 in Supporting Information S1, and the aerosol Pb and Pb isotope data are included in SI table S3 in Supporting Information S1. As of Feb. 2025, the data will also be available at Boyle et al. (2024a, 2024b). As of Nov. 2025, the data will also be available at the International GEOTRACES Intermediate Data Product 2025 hosted at <https://www.bodc.ac.uk>. Data labels are in English.

Acknowledgments
We thank the chief scientists Karen Casciotti, Phoebe Lam, and Greg Cutter for their excellent organization and execution of the field work and their cruise station map, as well as the field scientists hard work, high quality sample collection standards, and supporting information, in particular the Ocean Data Facility group for basic hydrographic data. We especially thank the GTC "clean team" sampling crew. We thank the captain, officers, and crew of the R/V Roger Revelle for their able and efficient ship operation. We thank Rick Kayser for his efforts in sample bottle preparation, archiving, instrument maintenance, and high purity reagent preparation at MIT, and Ryan Fraser for assistance in ID-TIMS analyses at MIT. We thank Rob Rember for cleaning sample bottles, and transferring the samples and the residual funding to us when his laboratory closed. We thank Reiner Schlitzer for his provision of Ocean Data View software (Schlitzer, 2020). MIT's work was supported by USA NSF grant OCE-1736996 to Edward Boyle and University of Alaska Fairbanks subcontract G11626 CR. TAMU's work was supported by NSF grant OCE-1737167 to Jessica Fitzsimmons and NTL-GRFP-1746932 to Nathan Lanning. None of the authors have any conflicts of interests to declare.

References

Bollhöfer, A., & Rosman, K. J. R. (2000). Isotopic source signatures for atmospheric lead: The southern hemisphere. *Geochimica et Cosmochimica Acta*, *64*(19), 3251–3262. https://doi.org/10.1016/s0016-7037(00)00436-1

Boyle, E. A., John, S., Abouchami, W., Adkins, J. F., Echegoyen-Sanz, Y., Ellwood, M., et al. (2012). GEOTRACES IC1 (BATS) contamination-prone trace element isotopes Cd, Fe, Pb, Zn, (and Mo) intercalibration. *Limnology and Oceanography: Methods*, *10*(9), 653–665. https://doi.org/10.4319/lom.2012.10.653

Boyle, E. A., Lanning, N., & Jiang, S. (2024a). Lead (Pb) concentrations and Pb isotope ratios (206Pb/207Pb, 208Pb/207Pb, 206Pb/204Pb) from Leg 1 (Seattle, WA to Hilo, HI) of the US GEOTRACES Pacific Meridional Transect (PMT) cruise (GP15, RR1814) on R/V Roger Revelle from September to October 2018 (Version 1) Version Date 2024-11-21 [Dataset]. *Biological and Chemical Oceanography Data Management Office (BCO-DMO)*. https://doi.org/10.26008/1912/bco-dmo.933318.1

Boyle, E. A., Lanning, N., & Jiang, S. (2024b). Lead (Pb) concentrations and Pb isotope ratios (206Pb/207Pb, 208Pb/207Pb, 206Pb/204Pb) from Leg 2 (Hilo, HI to Papeete, Tahiti) of the US GEOTRACES Pacific Meridional Transect (PMT) cruise (GP15, RR1815) on R/V Roger Revelle from October to November 2018 (Version 1) Version Date 2024-11-21 [Dataset]. *Biological and Chemical Oceanography Data Management Office (BCO-DMO)*. https://doi.org/10.26008/1912/bco-dmo.933383.1

Boyle, E. A., Lee, J.-M., Echegoyen, Y., Noble, A., Moos, S., Carrasco, G., et al. (2014). Anthropogenic lead emissions in the ocean – The evolving global experiment. *Oceanography*, *27*(1), 69–74. https://doi.org/10.5670/oceanog.2014.10

Boyle, E. A., Zurbrick, C., Lee, J.-M., Till, R., Till, C., Zhang, J., & Flegal, A. R. (2020). Lead and lead isotopes in the U.S. GEOTRACES east pacific zonal transect (GEOTRACES GP16). *Marine Chemistry*, *22*, 103892. https://doi.org/10.1016/j.marchem.2020.103892

Bushinsky, S. M., & Cerovečki, I. (2023). Subantarctic Mode water biogeochemical formation properties and interannual variability. *AGU Advances*, *4*(2), e2022AV000722. https://doi.org/10.1029/2022av000722

Chan, C.-Y., Zheng, L., & Sohrin, Y. (2024). The behaviour of aluminium, manganese, iron, cobalt, and lead in the subarctic Pacific Ocean: Boundary scavenging and temporal changes. *Journal of Oceanography*, *80*(2), 99–115. https://doi.org/10.1007/s10872-023-00710-8

Chen, J. H., Wasserberg, C. J., Von Damm, K. L., & Edmond, J. M. (1986). *The U-Th-Pb systematics in hot springs on the East Pacific rise at 21°N and Guaymas Basin* (Vol. 50, pp. 2467–2479). Geochim.Cosmochim. Acta.

Chow, T. J., & Patterson, C. C. (1962). The occurrence and significance of lead isotopes in pelagic sediments. *Geochimica et Cosmochimica Acta*, *26*(2), 263–308. https://doi.org/10.1016/0016-7037(62)90016-9

Chung, Y., Finkel, R., Bacon, M. P., Cochran, J. K., & Krishnaswami, S. (1983). Intercomparison of 210Pb measurements at GEOSECS station 500 in the northeast Pacific. *Earth and Planetary Science Letters*, *65*(2), 393–405. https://doi.org/10.1016/0012-821x(83)90178-4

Cutter, G. A., & Bruland, K. W. (2012). Rapid and noncontaminating sampling system for trace elements in global ocean surveys. *Limnology and Oceanography: Methods*, *10*(6), 425–436. https://doi.org/10.4319/lom.2012.10.425

Dirksen, R. J., Folkert Boersma, K., De Laat, J., Stammes, P., Van Der Werf, G. R., Martin, M. V., & Kelder, H. M. (2009). An aerosol boomerang: Rapid around-the-world transport of smoke from the december 2006 Australian forest fires observed from space. *Journal of Geophysical Research*, *114*(D21), D21201. https://doi.org/10.1029/2009JD012360

Edmond, J. M., Chung, Y., & Sclater, J. G. (1971). Pacific bottom water: Penetration east around Hawaii. *Journal of Geophysical Research*, *76*(33), 8089–8097. https://doi.org/10.1029/jc076i033p08089

Ewing, S. A., Christensen, J. N., Brown, S. T., Vancuren, R. A., Cliff, S. S., & Depaolo, D. J. (2010). Pb Isotopes as an Indicator of the Asian contribution to particulate air pollution in urban California. *Environmental Science and Technology*, *44*(23), 8911–8916. https://doi.org/10.1021/es101450t

Flegal, A. R., Gallon, C., Ganguli, P. M., & Conaway, C. M. (2013). All the lead in China. *Critical Reviews in Environmental Science and Technology*, *43*(17), 1869–1944. https://doi.org/10.1080/10643389.2012.671738

Flegal, A. R., Schaule, B. K., & Patterson, C. C. (1984). Stable isotope ratios of lead in surface waters of the central pacific. *Marine Chemistry*, *14*(3), 281–287. https://doi.org/10.1016/0304-4203(84)90048-3

Jensen, L. T., Wyatt, N., Landing, W., & Fitzsimmons, J. (2020). Assessment of the stability, sorption, and exchangeability of marine dissolved and colloidal metals. *Marine Chemistry*, *220*, 103754. https://doi.org/10.1016/j.marchem.2020.103754

Kawabe, M., & Fujio, S. (2010). Pacific Ocean circulation based on observation. *Journal of Oceanography*, *66*(3), 389–403. https://doi.org/10.1007/s10872-010-0034-8

Kelly, A. E., Reuer, M. K., Goodkin, N. F., & Boyle, E. A. (2009). Lead concentrations and isotopes in corals and water near Bermuda, 1780-2000. *Earth and Planetary Science Letters*, *283*(1–4), 93–100. https://doi.org/10.1016/j.epsl.2009.03.045

Lagerström, M. E., Field, M. P., Séguret, M., Fischer, L., Hann, S., & Sherrell, R. M. (2013). Automated on-line flow-injection ICP-MS determination of trace metals (Mn, Fe, Co, Ni, Cu and Zn) in open ocean seawater: Application to the GEOTRACES program. *Marine Chemistry*, *155*(0), 71–80. https://doi.org/10.1016/j.marchem.2013.06.001

Lanning, N., Jiang, S., Amaral, V. J., Mateos, K., Lam, P. J., Boyle, E., et al. (2023). Isotopes illustrate vertical transport of anthropogenic Pb by reversible scavenging within Pacific Ocean particle veils. *Proceedings of the National Academy of Sciences*, *120*(23), e2219688120. https://doi.org/10.1073/pnas.2219688120

Lee, J. M., Boyle, E. A., Echegoyen-Sanz, Y., Fitzsimmons, J. N., Zhang, R., & Kayser, R. A. (2011). Analysis of trace metals (Cu, Cd, Pb, and Fe) in seawater using single batch Nitrilotriacetate resin extraction and isotope dilution inductively coupled plasma mass spectrometry. *Analytica Chimica Acta*, *686*(1–2), 93–101. https://doi.org/10.1016/j.aca.2010.11.052

Lee, J.-M., Boyle, E. A., Gamo, T., Obata, H., Norisuye, K., & Echegoyen, Y. (2015). Impact of anthropogenic Pb and ocean circulation on the recent distribution of Pb isotopes in the Indian Ocean. *Geochimica et Cosmochimica Acta*, *170*, 126–144. https://doi.org/10.1016/j.gca.2015.08.013

Li, Z., England, M. A., Groeskamp, S., Cerovecki, I., & Luo, Y. (2021). The origin and fate of subantarctic Mode water in the southern ocean. *Journal of Physical Oceanography*, *51*, 2951–2972. https://doi.org/10.1175/JPO-D-20-0174.1

Marsay, C. M., Kadko, D., Landing, W. M., & Buck, C. S. (2022). Bulk aerosol trace element concentrations and deposition fluxes during the U.S. GEOTRACES GP15 Pacific Meridional Transect. *Global Biogeochemical Cycles*, *36*(2), e2021GB007122. https://doi.org/10.1029/2021GB007122

Matsumoto, K. (2007). Radiocarbon-based circulation age of the world oceans. *Journal of Geophysical Research*, *112*(C9), C09004. https://doi.org/10.1029/2007JC0040

McCartney, M. S. (1977). Subantarctic Mode water. In M. V. Angel (Ed.), *A voyage of discovery* (Vol. 1977, pp. 117–119). Pergamon.

McConnell, J. R., Lamorey, G. W., & Hutterli, M. A. (2002). A 250-year high-resolution record of Pb flux and crustal enrichment in central Greenland. *Geophysical Research Letters*, *29*(23), 2310. https://doi.org/10.1029/2002GL016016

McConnell, J. R., Maselli, O. J., Sigl, M., Vallelonga, P., Neumann, P., Anschütz, H., et al. (2014). Antarctic-wide array of high-resolution ice core records reveals pervasive lead pollution began in 1889 and persists today. *Nature Science Repts*, *4*(1), 5848. https://doi.org/10.1038/srep05848

NASA. (2020). *Global transport of smoke from Australian bushfires*. Global Modeling and Assimilation Office. Retrieved from https://gmao.gsfc.nasa.gov/research/science_snapshots/slides/Australia_fires_smoke.pdf

Nozaki, Y., Thomson, J., & Turekian, K. K. (1976). The distribution of 210Pb and 210Po in the surface waters of the Pacific Ocean. *Earth and Planetary Science Letters*, *32*(2), 304–312. https://doi.org/10.1016/0012-821x(76)90070-4

Nriagu, J. O. (1989). A global assessment of natural sources of atmospheric trace metals. *Nature*, *338*(6210), 47–49. https://doi.org/10.1038/338047a0

Patterson, C. C., & Settle, D. M. (1987a). Review of data on eolian fluxes of industrial and natural lead to the lands and seas in remote regions on a global scale. *Marine Chemistry*, *22*(2–4), 137–162. https://doi.org/10.1016/0304-4203(87)90005-3

Patterson, C. C., & Settle, D. M. (1987b). Magnitude of lead flux to the atmosphere from volcanoes. *Geochimica et Cosmochimica Acta*, *51*(3), 675–681. https://doi.org/10.1016/0016-7037(87)90078-0

Pinedo-Gonzalez, P., West, A. J., Tovar-Sanchez, A., Duarte, C. M., & Sanudo-Wilhelmy, S. A. (2018). Concentration and isotopic composition of dissolved Pb in surface waters of the modern global ocean. *Geochimica et Cosmochimica Acta*, *235*, 41–54. https://doi.org/10.1016/j.gca.2018.05.005

Reid, J. L. (1997). On the total geostrophic circulation of the Pacific Ocean: Flow patterns, tracers, and transports. *Progress in Oceanography*, *39*(4), 263–352. https://doi.org/10.1016/s0079-6611(97)00012-8

Reuer, M. K., Boyle, E. A., & Grant, B. C. (2003). Lead isotope analysis of marine carbonates and seawater by multiple collector ICP-MS. *Chemical Geology*, *200*(1–2), 137–153. https://doi.org/10.1016/s0009-2541(03)00186-4

Roskill Report. (1996). *The Economics of lead* (5th ed.). Roskill Information Services Ltd.

Sangster, D. F., Outridge, P. M., & Davis, W. J. (2000). Stable lead isotope characteristics of lead ore deposits of environmental significance. *Environmental Reviews*, *8*(2), 115–147. https://doi.org/10.1139/er-8-2-115

Schaule, B. K., & Patterson, C. C. (1981). Lead concentrations in the northeast pacific: Evidence for global anthropogenic perturbations. *Earth and Planetary Science Letters*, *54*(1), 97–116. https://doi.org/10.1016/0012-821x(81)90072-8

Schlitzer, R. (2020). Ocean data view. http://odv.awi.de

Sohrin, Y., Urushihara, S., Nakatsuka, S., Kono, T., Higo, E., Minami, T., et al. (2008). Multielemental determination of GEOTRACES key trace metals in seawater by ICPMS after preconcentration using an ethylenediaminetriacetic acid chelating resin. *Analytical Chemistry*, *80*(16), 6267–6273. https://doi.org/10.1021/ac800500f

Talley, L. D., Pickard, G., Emery, M., & Swift, J. (2011). *Descriptive physical Oceanography: An introduction* (6th ed.). Elsevier. ISBN 978-0-7506-4552-2.

Tang, W., Llort, J., Weis, J., Perron, M. M. G., Basart, S., Li, Z., et al. (2021). Widespread phytoplankton blooms triggered by 2019-2020 Australian wildfires. *Nature*, *597*(7876), 370–375. https://doi.org/10.1038/s41586-021-03805-8

Wu, J., Rember, R., Jin, M., Boyle, E. A., & Flegal, A. R. (2010). Isotopic evidence for the source of lead in the North Pacific abyssal water. *Geochimica et Cosmochimica Acta*, *75*, 460–468.

Zurbrick, C. M., Gallon, C., & Flegal, A. R. (2017). Historic and industrial lead within the Northwest Pacific Ocean evidenced by lead isotopes in seawater. *Environmental Science and Technology*, *51*(3), 1203–1212. https://doi.org/10.1021/acs.est.6b04666